Validation of MARS-KS code for critical heat flux on a single heater rod under inclined condition

Yujeong Ko, Hyoung Kyu Cho
Department of Nuclear Engineering, Seoul National Univ.,1 Gwanak-ro, Gwanak-gu, Seoul 08826
**Corresponding author: chohk@snu.ac.kr*

1. Introduction

Marine reactors are accompanied by various physical phenomena such as inclination and oscillation by sea waves. Several thermal-hydraulic characteristics can be changed by these physical phenomena. Therefore, the physical quantities used in land-based reactors under vertical conditions must be recalculated for the marine conditions. Among them, this paper focuses on CHF (Critical Heat Flux), which is an important criterion for nuclear reactor safety [1,2].

In this study, the inclined CHF correlation which was experimentally investigated in the previous study (Kim, 2021) is implemented into MARS-KS [3]. Then, it was validated that the experimental results of the CHF under inclination can be reasonably predicted by the improved code. Two experiments on a single heater rod conducted by Kim and Levy and Swan [4], were used for the validation.

This study would extend the applicability of MARS-KS to the safety analysis of a marine reactor.

2. MARS-KS Improvement

This section describes the modifications of MARS-KS for the implementation of the correlation and the simulation of the CHF experiments under inclination. They include the addition of a new fluid option for R134a, the annulus geometry correction factor for CHF Look-up Table, and the CHF correlation under inclination proposed by Kim.

2.1 R134a Properties addition in MARS-KS

The CHF correlation for the inclined geometry was developed based on the experimental database using water and R134a. In order to cover the available experimental conditions for thorough validation, the property information of R134a based on NIST data was added to MARS-KS.

2.2 CHF Correlation for annulus geometry

MARS-KS uses the Groeneveld Lookup Tables [5] for CHF prediction. It uses various correction factors to adjust various geometric and fluidic conditions. One of the factors is the annulus geometry correction factor. MARS-KS uses all the correction factors except for the annulus correction factor and thus, it was implemented in the present work. The concentric annuli correlation (Doerffer,1994) was used to compromise the geometrical differences between the rod heater experiments and tube experiments of look-up table [6]. The annulus correction comprises three correction factors; quality, gap size, and pressure correction as below.

$$CHF_{An} = CHF_{D=8} k_x k_\delta k_p \quad (1)$$

where CHF_{An} is the CHF for an annulus rod and $CHF_{D=8}$ is the CHF for a tube with an inner diameter of 8 mm, as predicted by the tube CHF look-up table (Groenveld, 1986). k_x accounts for quality effect;

for $x_c \leq 0.025$ mm

$$k_x = 0.81 \quad (2)$$

for $x_c > 0.025$ mm

$$k_x = 0.859 - 16.179\, x_c^{1.5} + 15.6 x_c^2 - 7.195 x_c^2 \ln x_c \quad (3)$$

where x_c denotes critical quality.

k_δ accounts for the gap effect;

for $\delta < 4.26$ mm

$$k_\delta = 0.2872 + 1.209\delta^2 - 1.156\delta^{2.5} + 0.2873\delta^3 \quad (4)$$

for $4.26 \leq \delta \leq 6.27$ mm

$$k_\delta = 1.2672 - 0.0298\delta \quad (5)$$

for $6.27 < \delta \leq 8.26\ mm$

$$k_\delta = 0.6663 + 64.374\, exp(-\frac{\delta}{1.242}) \quad (6)$$

for $\delta > 8.26\ mm$

$$k_\delta = 0.75 \quad (7)$$

k_p accounts for the pressure effect;

for $P < 3.30\ MPa$

$$k_p = 0.9 \quad (8)$$

for $3.3 \leq P \leq 10.5\ MPa$

$$k_p = 0.808 + 0.0278P \quad (9)$$

for $P > 10.5$ MPa

$$k_p = 1.1 \quad (10)$$

2.3 CHF correlation under inclination

The inclined CHF correlation for a single rod and single tube heater were proposed by Kim which considered the changes of relative direction between gravity and the flow direction under inclined condition, in both rod and tube geometries. The CHF mechanism can be distinguished into the DNB (Departure of nucleate boiling) and dry-out [7], and Kim suggested the Katto number ($\sigma\rho_l/G^2l_h$) of $5\cdot10^{-6}$ as the criterion of the two regime. The inclined CHF correlations are suggested for the DNB, dry-out regime, respectively, and Kim applied the CHF-regime determination function $\boldsymbol{R}$ in order to apply the correlation for each region without any discontinuity.

$$\boldsymbol{R} = \frac{1}{1+\left(\frac{\psi_{katto,TR}}{\psi_{katto}}\right)^4} \tag{11}$$

where $\psi_{katto} = \sigma\rho_l/G^2l_h$, $\psi_{katto,TR} = 5\cdot10^{-6}$, and subscript TR means transition.

The inclined CHF correlation consists of the correlation for DNB $\boldsymbol{f_{DNB}}$ and the correlation for dry-out $\boldsymbol{f_{DO}}$.

$$\frac{CHF_{IN}}{CHF_{VT}} = \boldsymbol{f} = (1-\boldsymbol{R})\cdot\boldsymbol{f_{DNB}} + \boldsymbol{R}\cdot\boldsymbol{f_{DO}} \tag{12}$$

where subscript IN and VT mean inclined and vertical respectively.

2.3.1 The correlation for DNB

The correlation for DNB is the function of non-dimensional numbers; $\frac{\rho_l}{\rho_v}$, $\boldsymbol{Fr_{DNB}}$, δ_{ij}, where ρ_l, ρ_v, $\boldsymbol{Fr_{DNB}}$,and δ_{ij} are saturated liquid density, saturated vapor density, Froude number for DNB region, and the geometry factor, respectively. To distinguish the buoyancy- and flow- dominant region, Kim reformed the non-dimensional numbers as $\boldsymbol{\Pi_{DNB}}$ [3].

$$\boldsymbol{f_{DNB}} \equiv \frac{CHF_{IN}}{CHF_{VT}} = 1+(-1)^{\delta_{ij}}\left[\left\{\left(\frac{(0.12\cdot\boldsymbol{\Pi_{DNB}})^2}{1+(0.12\cdot\boldsymbol{\Pi_{DNB}})^2}\right)^2 + \left(\frac{1}{(0.22\cdot\boldsymbol{\Pi_{DNB}})^{0.7}}\right)^2\right\}^{\frac{1}{2}} - 1\right], \tag{13}$$

where

$$\boldsymbol{Fr_{DNB}} \equiv \frac{G}{\rho_l\sqrt{gcos\varphi D(\Delta\rho/\rho_l)}}, \tag{14}$$

$$\boldsymbol{\Pi_{DNB}} = \left(\frac{\rho_l}{\rho_v}\right)^{0.5}\boldsymbol{Fr_{DNB}}, \tag{15}$$

$$\delta_{ij} = \begin{cases} 1\ (rod) \\ 0\ (tube) \end{cases} \tag{16}$$

2.3.2 The correlation for dry-out

The correlation for dry-out is the function of non-dimensional number; $\frac{\rho_l}{\rho_v}$, $\frac{\boldsymbol{l_{heat}}}{\boldsymbol{d_{heat}}}$, $\boldsymbol{Fr_{DO}}$, and a, b, c, where $\boldsymbol{l_{heat}}$, $\boldsymbol{d_{heat}}$, $\boldsymbol{Fr_{DO}}$ and a, b, c are heated length, heated equivalent diameter, Froude number for dry-out region, and the geometry factors, respectively [3].

$$\boldsymbol{f_{DO}} \equiv \frac{CHF_{IN}}{CHF_{VT}} = 1+\left(\frac{\rho_l}{\rho_v}\right)^{-0.7}\left(\frac{\boldsymbol{l_{heat}}}{\boldsymbol{d_{heat}}}\right)^a \left(\boldsymbol{Fr_{DO}}^{3.2}-b\right)\exp(-(\boldsymbol{Fr_{DO}}+7.5)^c), \tag{17}$$

where

$$\boldsymbol{Fr_{DO}} \equiv \frac{Gx_{eq}}{\rho_v\sqrt{gDcos\varphi\left(\frac{\Delta\rho}{\rho_v}\right)}}, \tag{18}$$

$$(a,b,c) = \begin{cases} (1.15,\ 0,\ 0.9)\ for\ rod \\ (1.30,\ 100,\ 0.8)\ for\ tube \end{cases} \tag{19}$$

The applicable ranges of the correlation are summarized in Table 1 [3].

Table 1: Applicable ranges of CHF correlation

L/D D_{hy} [mm] D_{heat}[mm]	Pressure [MPa]	Mass flux [kg/m^{2}s]	Quality [-]
48 ~ 125 6.3 ~ 8.5 16.6 ~ 22.3	7 ~ 18	300 ~ 2500	-0.5 ~ 0.9

2.4 CHF detection in MARS-KS

The CHF condition for a given condition was detected by comparing the imposed heat flux and the CHF value calculated using the correlation and the look-up table. For this, the wall heat flux was increased gradually. When the heat transfer from the convective boundary became larger than or equal to the calculated value, the condition was selected for the CHF point. Fig. 1 show an example of the CHF determination. It is clearly shown that the heat transfer from the convective boundary suddenly dropped when the two lines crosses and consequently, the heat transfer suddenly deteriorated. This procedure was repeated for all heat structure nodes and the CHF occurred in the node at the end of the heated channel for all cases.

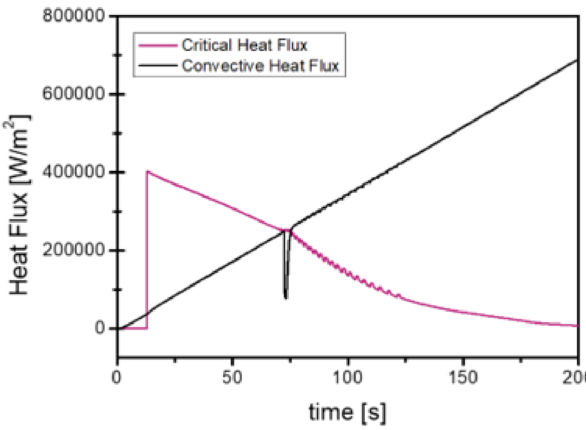

Fig.1. Example of the CHF detection in MARS-KS

3. Verification & Validation

In this section, the V&V of the modified MARS-KS was performed by simulating test facilities of Kim [3] and Levy and Swan[4]. The experiment platform by Kim is called NEOUL-R.

3. V&V against NEOUL-R [3] (R-134a test)

A MARS-KS nodalization that can simulate the test section geometry of the experiment by Kim was presented in Fig.2. The schematic diagram of the test section is shown in Fig.3. It consists of a heater rod with

9.5 mm diameter and 800 mm heated length which was installed inside of a pipe, and the outer surface of the rod allowed heat transfer through convection.

For verification, the calculated ratio between inclined CHF and vertical CHF according to Fr_{DNB} and Fr_{DO} is compared with the stand-alone correlation in Fig.4. The region near zero value of Fr_{DO}, the predicted values showed larger values than the correlation. This is caused by the interpolation between the DNB and dry-out correlations and it was confirmed that the implemented interpolation scheme works properly according to the f value. The calculated result by developed MARS-KS code indicated good agreement with the correlation.

The result of calculating all inclined CHF according to experimental data is shown in Fig.5. It exhibited better agreement with the experimental data after implementation within a standard deviation of 8.4 % and maximum error of 32.1 %, especially at high pressure.

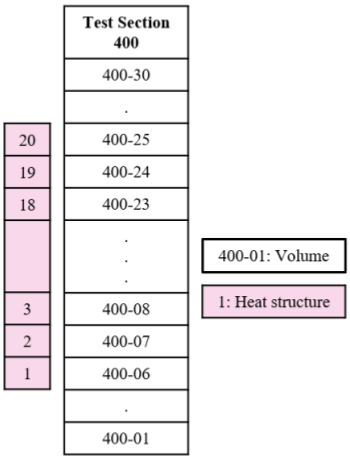

Fig.2. Nodalization of NEOUL-R and Levy and Swan experiment in MARS-KS

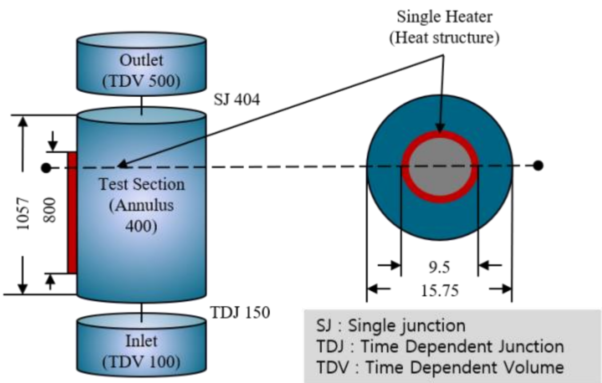

Fig.3. Schematic diagram of NEOUL-R experiment loop

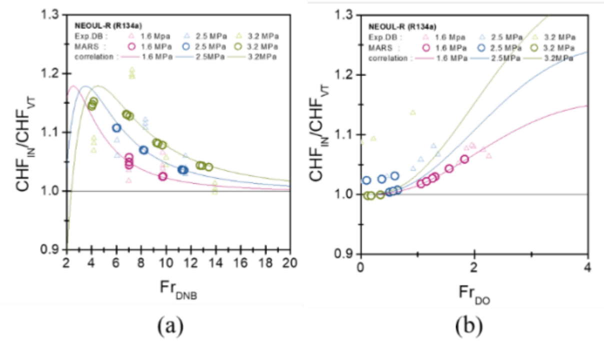

Fig.4. Comparison of CHF_{IN}/CHF_{VT} of MARS-KS calculation and NEOUL-R experiment due to (a) Fr_{DNB} (b) Fr_{DO}

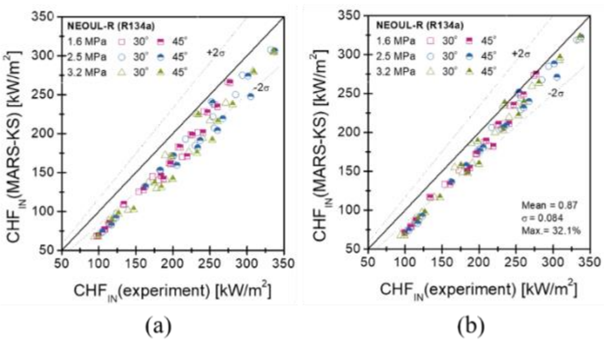

Fig.5. The inclined CHF of MARS-KS calculation due to inclined CHF of NEOUL-R experiment (a) before implementation (b) after implementation

3.2 V&V against Levy and Swan [4] (water test)

The MARS-KS nodalization for the test section of the experiment by Levy and Swan was presented in Fig.2. The schematic diagram of the test section is shown in Fig.6. It consists of a heater rod with 13.72 mm diameter and 2794 mm heated length which was installed at the center of a pipe.

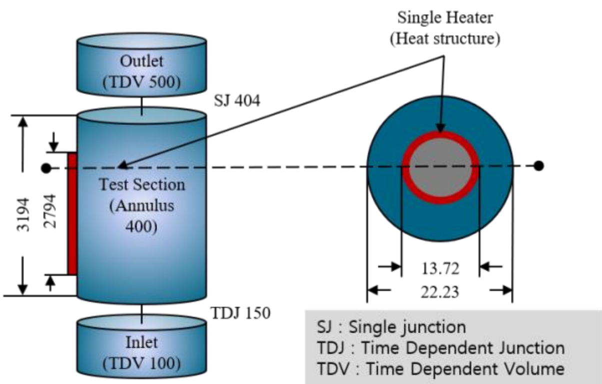

Fig.6. Schematic geometry of Levy and Swan experiment loop

The predicted result of the CHF ratio is shown in Fig.8 with the stand-alone correlation and the experimental data. It was verified that MARS-KS reproduced the correlation accurately. Then, the calculation results are compared with the experimental results in fig. 9. It exhibited better agreement with the experimental data after implementation within a standard deviation of 4.70 % and maximum error of 17.5 %. It was confirmed that the predictability of MARS-KS was improved after the modification.

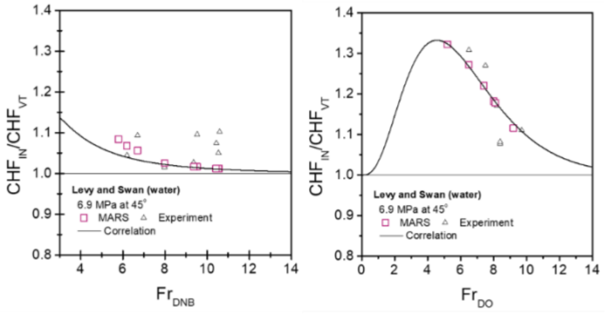

(a) (b)

Fig.8. Comparison of $\mathrm{CHF_{IN}}/\mathrm{CHF_{VT}}$ of MARS-KS calculation and NEOUL-R experiment due to (a) $\mathrm{Fr_{DNB}}$ (b) $\mathrm{Fr_{DO}}$

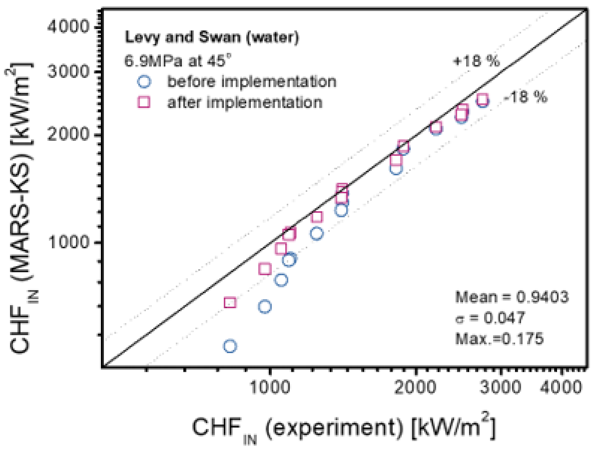

Fig.9. The inclined CHF of MARS-KS calculation due to the inclined CHF of Levy and Swan experiment before and after implementation

4. Conclusion

In this study, the CHF correlation for a inclined heater was applied to the MARS-KS code and the validity of the implementation was confirmed by simulating two test facilities. Through this work, the CHF prediction capability of MARS-KS under inclined conditions is improved with the new correlation and the annulus correction factor.

In this paper, only validation of a single rod heater was conducted. Therefore, validation for a single tube heater should be carried out. After the validation for the inclined condition is completed, a model for rolling conditions, which is another physical phenomenon of the marine environment, will be tested.

ACKNOWLEDGEMENT

This work was supported by the Nuclear Safety Research Program through the Korea Foundation Of Nuclear Safety (KoFONS) using the financial resource granted by the Nuclear Safety and Security Commission (NSSC) of the Republic of Korea. (No, 2003005)

REFERENCES

[1] Yan, B. H. "Review of the nuclear reactor thermal hydraulic research in ocean motions." Nuclear Engineering and Design 313 (2017): 370-385.
[2] Tian, Zhen, et al. "Flow boiling heat transfer under marine motions: A comprehensive review." Annals of Nuclear Energy 143 (2020): 107455.
[3] Geon-Woo Kim. Experimental Investigation of Critical Heat Flux on a Single Heater Rod under Inclined and Rolling Conditions / Geon-Woo Kim [electronic Resource] (2021). Web.
[4] Levy, S., & Swan, C. L. (1959). Performance--two-phase Pressure Drop, Burnout, and Hydraulic Oscillation of an Inclined Test Section with Net Steam Generation at 1000 PSIA (No. GEAP-3228 (Rev. 1)). General Electric Co. Atomic Power Equipment Dept., San Jose, Calif..
[5] Groeneveld, D. C., S. C. Cheng, and T. Doan. "1986 AECL-UO critical heat flux lookup table." Heat transfer engineering 7.1-2 (1986): 46-62.
[6] Doerffer, S., et al. "A comparison of critical heat flux in tubes and annuli." Nuclear Engineering and Design 149.1-3 (1994): 167-175.
[7] Katto, Yo, and M. Shimizu. "Upper limit of CHF in the saturated forced convection boiling on a heated disk with a small impinging jet." (1979): 265-269.